



## Transferring momentum: Novel drop protection concept for mobile devices

Kevin Hughes<sup>a,\*</sup>, Rade Vignjevic<sup>b</sup>, Fergal Corcoran<sup>c</sup>, Omkar Gulavani<sup>d</sup>, Tom De Vuyst<sup>a</sup>, James Campbell<sup>a</sup>, Nenad Djordjevic<sup>a</sup>

<sup>a</sup> Structural Integrity Theme/Mechanical and Aerospace Engineering, NSIRC, Brunel University London, Cambridge, CB21 6AL, UK

<sup>b</sup> Structural Integrity Theme/Mechanical and Aerospace Engineering, Brunel University London, UB8 3PH, UK

<sup>c</sup> Logitech Ireland Services Ltd, Cork, Ireland

<sup>d</sup> Applied Mechanics, School of Aerospace, Transport and Manufacturing, Cranfield University, Bedford, MK43 0AL, UK

### ARTICLE INFO

#### Keywords:

Drop impact simulation  
Impact tolerance of portable electronic devices  
Protection concept development  
Virtual Design/Testing of Protective Packaging

### ABSTRACT

Dropping a tablet (or mobile phone) can be extremely costly, as loss of functionality, visible body damage, screen delamination and failure are all too familiar outcomes. This paper discusses the analysis led design of a novel passive protection concept, capable of isolating a device from the primary impact, and is also insensitive to impact angle and device dependent features.

A high fidelity finite element model of an iPad Air was used to develop the BLOK™ protection concept, which utilises different grades of elastomer, optimised internal castellation geometry and a high stiffness backplate. Sensitivity studies include the influence of glass properties, screen bonding and impact angle on the robustness of the numerical predictions, whereby quantitative comparisons with experimental data in terms of metal body damage (location, size) and accelerometer data were used.

Explicit finite element analysis verifies the effectiveness of decoupling the tablet from the impact loads, as resultant acceleration for unprotected versus protected was reduced by ~76% (2152 g vs 509 g), and consistent with ~74% reduction observed through testing (1723 g vs 447 g). For the protected tablet, simulation predicted displacements within 6%, with peak acceleration overestimated by 14%, and attributed to overestimating elastomer stiffness at full compression and its subsequent unloading.

Final validation demonstrated device independence by protecting an iPad Air 2™ (with significantly different internal structure to Air™), against corner and short edge impacts. The concept developed resulted in a product to market with a mass of 165 g (~36% tablet mass), providing protection from a 1.8 m drop onto concrete, far exceeding MIL-STD-810G requirements.

### 1. Introduction

The mobile electronic device market is buoyant with many products available at differing price levels, functionality, size and operating system. From quarterly audits published by Apple™, over 337 million unit sales worldwide have been sold since iPad launch in 2010 [1]. As a result of its popularity, this paper is based upon demonstrating the feasibility of a novel protection concept using an iPad Air as the reference configuration for the testing and simulation campaign.

As mobile devices evolve, increased functionality and performance lead to reductions in size and weight, with the Air (launched November 2013) having a 211–253 g mass saving over 1st generation iPad (launched April 2010) [2]. As a consequence of reducing mass (including metal body thickness), impact resistance and durability of the protective outer glass screen and /or underlying LCD are the most damage sensitive components if dropped onto a hard surface. After

reviewing the literature, no papers were found on the application of numerical simulation to tablets, with only a few papers related to phone drops. Therefore, this review was extended to consider impact loading of other electronic devices (laptops and PDAs), in addition to papers related to packaging design (for protection during transit). A chronological summary of relevant papers is presented in Table 1.

Summarising the findings from Table 1;

1. For mobile phones, flexing of LCD screen/PCB are common modes of failure, as shock induced vibrations result in differential bending and extreme cyclic stress, resulting in crack propagation/separation under low cycle fatigue.
2. Repeatability of drop tests is important, as slight deviations in impact angle can significantly affect impact forces/accelerations.
3. Corner drop tests are more repeatable and result in significant damage. However, other studies report horizontal edge impacts being

\* Corresponding author.

E-mail addresses: [kevin.hughes@brunel.ac.uk](mailto:kevin.hughes@brunel.ac.uk) (K. Hughes), [fcorcoran@logitech.com](mailto:fcorcoran@logitech.com) (F. Corcoran).

**Table 1**  
Review of electronic device drop simulation and testing, including protective packaging.

Author	Date	Conclusions
Suhir [20]	1994	Analysed the dynamic response of a rectangular plate (e.g. liquid crystal display) and demonstrated that plate thickness and clamping could improve failure strength.
Nagaraj [21]	1997	Applied numerical simulation to determine PCB integrity by assessing vibrational mode shapes and identifying maximum displacements and potential impact points within case.
Goyal [22]	1999	Identified thin-walled clamshell phone cases may not have sufficient structural rigidity to resist impact loading. In 2000, battery integrity was assessed, which identified a problem with manufacturing. Author proposed an automated drop testing method to improve repeatability.
Goyal [23]	2000	Battery integrity was assessed, which identified a problem with manufacturing. Author proposed an automated drop testing method to improve repeatability
Low [24]	2001	Modelling, simulation and test correlation for 0.6, 0.8 and 1.2 m drop heights of hi-fi products onto concrete. Numerically, difficulties encountered with accuracy of material properties and small time steps, resulting in a sub modelling approach recommended for damage assessment of internal components.
Lim [25]	2002	Varied impact height (0.55–1 m) and angle for drop testing an electronic pager, where LCD represented with solid elements (including glass), equivalenced to membrane elements representing the lens (to extract surface strains). Correlation with force transducers, accelerometers and strain gauges showed importance of minimising idealisation errors, with vibration of lens/LCD identified as cause of failure due to cyclic strains.
Seah [26]	2002	Supported observation that impact angle and device specific design are important parameters, strongly influencing PCB failure, where shock induced vibration results in differential bending and extreme cyclic stress, resulting in crack propagation/separation under low cycle fatigue.
Lim [27], Lim [28]	2002, 2003	Impact angle sensitivity to phone/PDA devices, identifying maximum forces for direct vertical/horizontal impacts to be 2–5 times higher than for oblique impacts. Loading heavily influenced by dimensions and device composition. If internal components are in direct contact with outer case, loading directly transmitted and is severely damaging.
Low [29]	2003	Developed simplified models for hi-fi, hard disk drive and irons to predict transient impact response through equivalent spring-mass systems. Influence of mass on the benefits of providing a cushioning buffer (Expanded polyethylene) to reduce shock loading was investigated, which controlled spring back of the buffer material.
Low [30]	2004	Utilised a sub-modelling approach for 0.5 m drop impact analysis of a 29" TV, where the local model concentrated on the detailed analysis of four tube attachment screws. Increasing the radius of curvature at the impact point is beneficial in reducing stress concentrations.
Lye [31]	2004	Applied Genetic algorithms to optimise protective packaging buffers using bio-degradable materials (paper pulp and starch). Testing conducted on six configurations resulting in agreement within 12%.
Yi [32]	2005	Applied a Design of Experiments to optimise Expanded polystyrene monitor packaging, using an automated optimisation framework reducing design cycle from weeks to days. Approach is complex and worked well for homogeneous packaging, which could be applied to tablet protection.
Wang [33]	2005	Reviews impact response of different devices including styrofoam modelling for a TV and a PCB with an interference fit. Conclusions general, with recommendations made regarding importance of simplify material geometry (due to long CPU times/mesh distortions), definition of contact and material model accuracy.
Tan [34]	2005	Investigated simplified and detailed drop test modelling of printed circuit board (PCB), integrated circuits (IC) and interconnecting solder balls to determine PCB deflection and solder stresses. Large variation in predicted stress observed due to complex interaction between components, necessitating detailed solid element models for correlation.
Cadge [35]	2006	Considered failure of joints through a 1 m drop of an optical computer mouse. Approach adopted included sub-modelling, whereby system level time histories were extracted and applied to a detailed joint model using ABAQUS. Modelling approach identifies a location for possible joint failure/detail stresses, but no experimental validation provided.
Shan [36]	2007	Developed an analytical model for a rigid body impacting multiple times onto a viscoelastic surface. Subsequent impacts can occur at multiple case locations and may be more severe (in terms of contact force), due to random angles of impact.
Pan [37]	2007	Simulation and test correlation for 0.5 and 1.0 m drop tests of TFT-LCD monitors. Key components modelled, including expanded polyethylene foam packaging. Screen simplified (10 layers represented by two glass substrates), with $E = 64$ GPa and $\sigma_y = 60$ MPa. Corner, three edge and six face orientation tests performed, whereby accelerations and dynamic strains agreed within 20% of test. Face impacts deemed critical, resulting in failure of the plastic housing around an attachment point.
Yu [38]	2010	Out of plane bending and clamping arrangements of a mobile phone PCB board investigated, where Digital Image Correlation calculated accelerations and displacements from high-speed cameras. FEA overestimated deflections, attributed to uncertainties in damping and use of linear elastic constitutive models (no energy losses).
Grewolls [39]	2010	Numerical simulation at NOKIA™ identified a corner drop, with two or more subsequent impacts, resulted in maximum stress. Time histories sensitive to small changes in impact angle, and deemed more critical than geometric or material non-linearities. Damage sensitive components include the display and soldered connections.
Hwan [9]	2011	Phone drop testing showed damage to inner LCD was common in screen up/face down configurations, where the survival rate is influenced by glass, adhesive used, shape of housing and internal packaging. Horizontal drops extremely damaging due crack initiation in the glass.
Altair Engineering [40]	2013	(Press release) Altair and LG Electronics (Korea) launched an automated drop test simulation process within Hyperworks™, to streamline FE modelling, set-up and post-processing of drop simulations, allowing engineers to reduce simulation time to 24 hours.
Blanco [41]	2015	Numerical optimisation of packaging for refrigerators against $2.2\text{ms}^{-1}$ impacts. Modelling packaging resulted in over 3.3million tetrahedral elements resulting in good agreement to test for refrigerator damage. Analysis led design led to packaging modifications.

critical for PCB/screen.

- Sub-modelling recommended when undertaking impact damage assessment of smaller, internal components (such as solder attachments on PCBs). Solid element formulations align better with test when compared to shell formulations.
- LCD/Glass models are extremely simplified, due to unknown material parameters and CPU run time considerations. Screen survivability is influenced by the type of glass, adhesive bonding, shape of housing and internal packaging arrangements.
- Impact angle and device specific geometry (including materials) are important parameters, strongly influencing (PCB) failure.
- Case geometry important, as local load alleviation may occur through case deflections.
- Subsequent impacts after initial rebound may be more severe (in terms of contact force), due to differing angles of impact and multiple case contact points.

At the time of this research, no published data on experimental or numerical drop analyses related to tablets was found. As there are no precedents for numerical modelling of a tablet in the open literature,

this paper presents the development of a validated, simulation driven design process, used to develop a manufacturable solution to protect any mobile device from drop heights up to 1.8 m onto a concrete, validated through a series of repeatable drop tests. Modelling assumptions, together with identification and treatment of sources of uncertainties, including the influence of glass properties, screen bonding and impact angle will be presented

Quantitative comparisons with experimental data in terms of metal body damage (location, size) and accelerometer data were used for validation. This paper concludes with the development of a proof of concept, prototype design and experimental testing of a protection system capable of isolating a tablet from the primary impact, resulting in a product to market.

## 2. Initial 1.8 m drop testing

For initial testing, a single impact location onto a steel surface (the corner to the right of the home button), was used to drive development of the numerical model and refine test setup. This location was chosen to compare protection concepts and once the preferred concept was selected, additional impact locations were tested numerically and experimentally.

A Phantom Mira320S High Speed Cameras with a frame rate of 3600 fps at 1280 × 720 resolution was used to capture front (screen) and a second 1000 fps camera for side orientations.

A triaxial 10 V excitation DC accelerometer (Model 53, Measurement Specialties™) with a measurement range ± 2000 g and frequency response of 4.5 KHz in the local Z direction and 2.5 KHz in local X and Y directions was bonded along tablet centreline, 65 mm above the Apple™ logo and 175 mm above the home button. This location was chosen due to concerns over the integrity of bonding directly to the rear Apple™ logo. The local accelerometer XY plane was defined to be in the plane of the metal body, with the local X axis aligned with the longitudinal tablet axis.

Defining a global XZ coordinate system to be in the plane of the glass screen, impact angles were quantified post impact. Also provided in Fig. 1 are filtered and unfiltered resultant accelerations corresponding to  $\Delta\theta_z = +2.08^\circ$  and  $\Delta\theta_x = -1.64^\circ$ , acquired via Labview through a NI USB-6212 BNC DAQ. Z-deviations,  $\Delta\theta_z$ , were measured relative to dotted points running corner to corner, where their intersection defines tablet centre. (i.e. If the normal of the impacted surface aligns with the dots, this would denote a perfect corner drop). The X-deviation,  $\Delta\theta_x$ ,

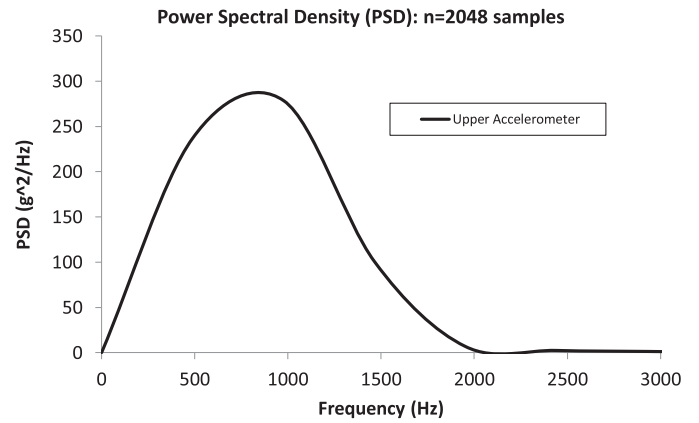


Fig. 2. Power spectral density for upper accelerometer.

means the tablet was tilted slightly backwards.

All signals filtered using a 4th order zero-phase Butterworth filter with 2.5 kHz cut-off, which based on the Power Spectral Density (PSD) of the raw data, shows the energy of the signal is sub 2 kHz, Fig. 2. For validation, the average (simulation) peak acceleration across 2.5, 3.5 and 5.5 KHz cut off frequencies was  $\sim 1723 \pm 39$  g, with a Full Width at Half Maximum (FWHM) duration of  $\sim 0.43$  ms. This impact resulted in metal body deformation, partial outer glass debonding and failed LCD screen, Fig. 3.

## 3. Finite element representation

This section describes geometry generation, the level of idealisation, element formulation and material models, including boundary conditions and extraction of acceleration time histories. Development was exploratory in nature to quantify model robustness and accuracy, using LS-DYNA v971 double precision solver [2].

### 3.1. Deconstructing an iPad Air

Thickness data for thirty components were measured using a Creaform hand scanner (Fig. 4 and Table 2). The majority of components (batteries, screen, speakers, etc) are regular in shape, trivial to mesh and directly bonded to metal body. Non-structural components (e.g. magnets) were represented by assigning additional mass.

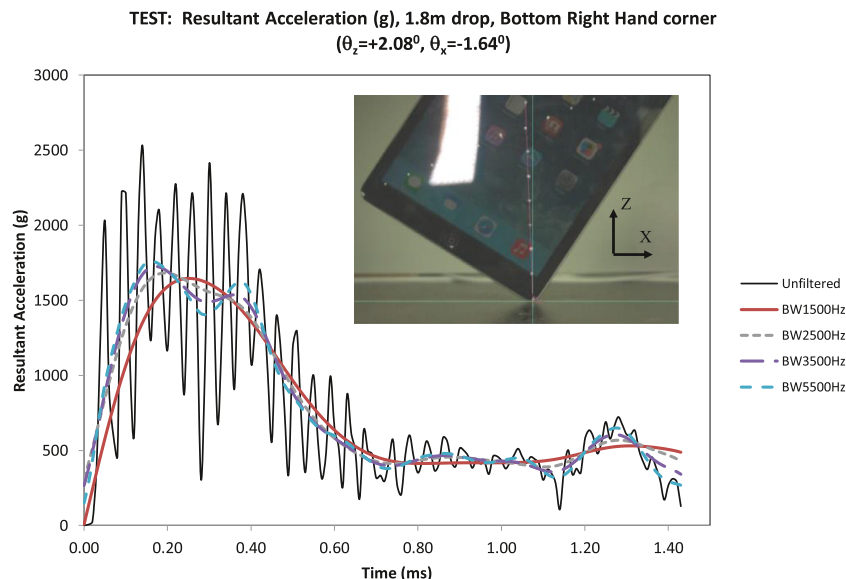


Fig. 1. Filtered resultant acceleration (g) using various Butterworth filters for a 1.8 m Air drop onto steel ( $\Delta\theta_z = +2.08^\circ$  and  $\Delta\theta_x = -1.64^\circ$  relative to a “perfect” corner drop).

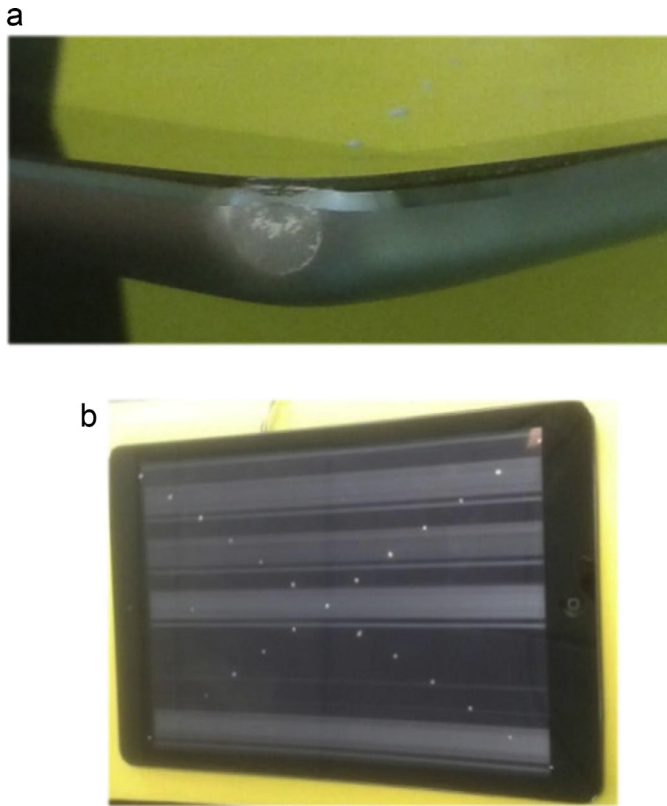


Fig. 3. Failure modes from a 1.8 m Air drop onto steel. Damage includes (a) plastic deformation and partial glass debonding and (b) a non-functioning LCD.

The metal body is milled from a single piece of aluminium, has complex geometric features, varying thicknesses and fillet radii. Each corner is different and requires precise geometric representation and careful meshing if model accuracy is to be independent of impact orientation.

The LCD is supported by steel (0.25 mm) and plastic (1.90 mm) surrounds, bonded and secured to the metal body by four corner screws (Fig. 5). The outer glass is a high resilience Aluminosilicate, bonded to the metal body via a 0.44 mm adhesive layer. An important modelling feature was the chamfered outer edge, (which provides edge protection) and may under certain impact conditions, form the initial contact point and directly load the outer glass.

### 3.2. Element selection

As the primary metric for validation was an accelerometer bonded

Table 2  
Variation in thickness of key components in an iPad Air.

Part	Thickness ( ± 0.03 mm)
Outer Glass Screen	0.60
Adhesive (between screen and metal body)	0.44
LCD Glass	1.00
LCD Metal Surround	0.25
LCD Plastic Surround 1	1.90
LCD Plastic Surround 2	0.90
Battery	2.65
PCB Main	2.50
Adhesive (between PCB and Metal body)	0.50
Speakers	1.20
Lightning Support Connector	0.75

to the case, the time histories would be highly influenced by outer case stiffness and internal packaging/bonding (which reinforces the case locally). Due to this non-uniform case stiffness, key internal components (and contact) were necessary modelling details to include.

Discretisation required thin shell, thick shell and solid elements, where assignment was determined by component geometry, the underlying material and structural response to be captured and time step considerations. For LS-DYNA element functionality and formulation, the reader is referred to [3,4].

In general:

- Shell elements assigned to thin components, such as the LCD support tray ( $t = 0.25$  mm). Offset contact types ensure connectivity between varying shell geometric definitions and external faces of adjacent components.
- Solid/Hexahedral elements (first and second order) were used to discretise complex geometries (to maintain control over accuracy and aspect ratios) and allow for 3D stress states.
- Thick Shell Elements (TSHELLS) represent through thickness and bending response of intermediate thickness components, utilising three to five through thickness integration points. TSHELLS eliminates the need for contact offsets, as volume is modelled explicitly using the same nodal definition as solid elements.

Model development was incremental and several iterations needed to demonstrate both accuracy and efficiency. For example, in order to verify the number of elements through thickness for the metal case, a benchmark implicit bending simulation allowed element formulation/size to be assessed against an analytical solution, resulting in the final element choices presented in Table 3. The converged model contained 212 K elements and took ~3 h on 8CPUs (Intel i7-4810MQ) to simulate 1.4 ms after impact.

Based upon the geometry, penalty based contact algorithms (Surface

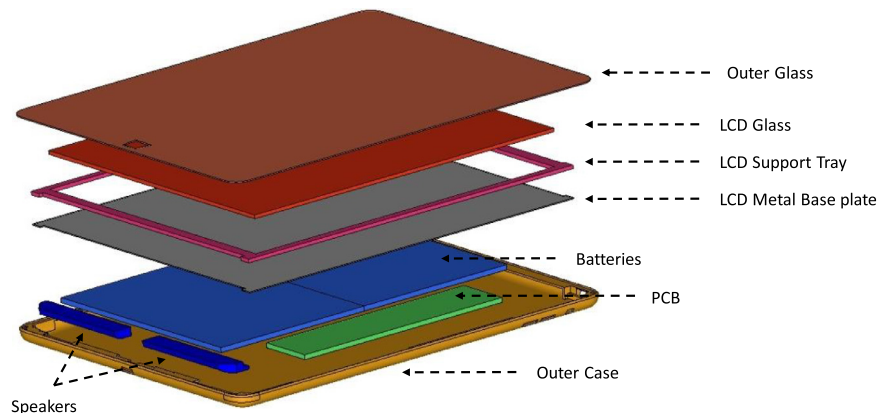


Fig. 4. iPad Air: exploded view.

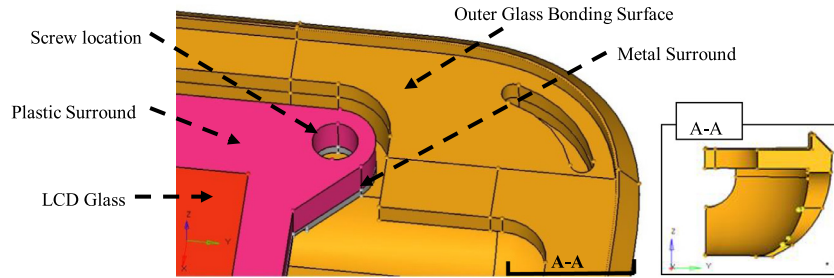


Fig. 5. Earphone socket corner, detailing one of the LCD surround attachment points and bonding area for outer glass. Inset image shows varying metal body thickness and chamfered outer edge.

to surface) and (tied surface to surface) were defined to represent general contact between interacting parts and also account for bonded connections. Appropriate offsets were defined to scale slave and master effective thicknesses to take into account gaps between components. Definition of master and slave entities were through dedicated contact surfaces extracted on faces of TSHELLS/SOLIDS, resulting in fifteen contact definitions.

### 3.3. Material types

Four primary material models assigned (Table 4), with elastic properties assumed for all internal components, with equivalent stiffness of Al6063-T6, as exact material types are not disclosed by Apple™. This approximation was reasonable as these components could not deform, due to tight internal packaging and bonding. A rigid material was used to define the impact surface and represent the inertia of the accelerometer.

As capturing localised damage to the outer metallic case, Johnson-Cook parameters were determined from testing using coupons extracted from an iPad Air. Due to the brittle nature of glass, a Johnson–Holmquist ceramic model was required and discussed in more detail in Section 3.4.

### 3.4. Outer glass constitutive model

As Apple™ does not disclose materials/suppliers used, outer glass and LCD specification are unknown. The glass was assumed to be aluminosilicate and based on manufacturer data for Gorilla Glass™, due to its widespread application in phones, tablets and laptops [5]. The thermal and chemical treatment applied provides screen resilience through a compressive preload generated in the top glass layers, which minimises surface cracks opening.

The Johnson–Holmquist Ceramic constitutive model (MAT110), is suited for modelling brittle materials, including ceramics and glass [6]. Evolution of hydrostatic pressure, which affects material strength, is

accounted by an equation of state, coupled with a damage state variable to track damage accumulation.

Using five material (A, B, C, n and m) and two damage constants ( $d_1$ ,  $d_2$ ), allows calculation of uniaxial strength at a given state of damage, by interpolating between intact and complete failure stress states using a scalar damage parameter,  $D$ , calculated per cycle. (i.e.  $d_1$  controls the rate at which damage accumulates, which if set to zero, means full damage occurs in one timestep, i.e. instantaneously).

$$\sigma^* = \sigma_{intact}^* - D(\sigma_{intact}^* - \sigma_{fracture}^*) \tag{1}$$

Where

$$\begin{aligned} \sigma_{intact}^* &= A(p^* + T^*)^n [1 + C \ln \dot{\epsilon}] \\ \sigma_{fracture}^* &= B(p^*)^m [1 + C \ln \dot{\epsilon}] \end{aligned} \tag{2}$$

$$D = \sum_{cycle} \frac{\Delta \epsilon^p}{\epsilon_p^f} = \sum_{cycle} \frac{\Delta \epsilon^p}{d_1 (p^* + T^*)^{d_2}} \tag{3}$$

Required strength ( $T$ ) and pressures ( $\sigma$  and  $p$ ) are normalised by the equivalent stress and pressures at the Hugoniot Elastic Limit (HEL) [3].

$$\sigma^* = \frac{\sigma}{\sigma_{HEL}}; \tag{4}$$

$$p^* = \frac{p}{p_{HEL}}; \tag{5}$$

$$T^* = \frac{T}{\sigma_h} \tag{6}$$

Specialist dynamic tests are required to populate this material model and beyond the scope of this study. Therefore, material parameters presented in Table 5 are open source for silica based glass, which matches the 30.4 GPa shear modulus of Gorilla Glass™ [5]. In light of this approximation, this constitutive model allows for element deletion (based on a user defined plastic failure strain), which could be tuned against test to infer the likelihood of failure (not the mode/extent), when assessing effectiveness protective concepts.

Table 3  
Element formulation and size, resulting in over 211 K elements for converged model.

Component	Element type	Integration rule	Average element size (mm)	# Nodes	# Elements	Mass (g)
Case	Impacting Corner – SOLID	FI	0.65	3766	2799	107.6
	Main Case – SOLID	FI	1.00	183,585	125,419	
	Upper Strip – SOLID	FI	0.35	9339	5082	
PCB	TSHELL	FI	2.25	1908	1144	18.5
BATTERIES	SOLID	FI	2.25	11,232	7144	149.5
LCD metal tray	TSHELL	RI	2.00	17,204	8412	22.8
LCD plastic surround	SHELL	FI	2.00	5308	2892	18.0
LCD GLASS	SOLID	FI	2.00	30,492	22,344	66.1
Speaker(s)	SOLID	FI	2.00	1944	1182	18.5
Outer glass	SOLID	FI	1.50	53,727	35,270	62.1
Rigid floor	SHELL	RI	3	33,768	33,400	NA
Accelerometer		Not applicable (NA)				4.2
<b>TOTAL</b>				<b>318,505</b>	<b>211,688</b>	<b>467.3</b>

**Table 4**  
Overview of the main constitutive models assigned.

Material model	Material	Johnson cook parametes	Youngs' modulus (MPa)	Poisson's ratio
*MAT_SIMPLIFIED_JOHNSON_COOK - Outer Case	Al6063-T6	A = 174.02 MPa B = 142.07 MPa n = 0.2196 c = 0		
*MAT_JOHNSON_HOLMQUIST_CERAMIC - Outer Glass - LCD Glass	Alumina Silicate thin sheet glass		71,700–73,000	0.22
*MAT_ELASTIC - LCD Metal Tray	Steel		210,000	0.33
- LCD Plastic Support	PC/ABS, Chimei PC-365		2200	0.44
- Batteries	Assume Al6063-T6		69,500	0.33
- PCB Main	Assume Al6063-T6		69,500	0.34
- Speakers	Assume Al6063-T6		69,500	0.34

From stability considerations, a strain to failure of 12% was required to prevent excessive distortions affecting run completion (and run time considerations). Using the definition of numerical accelerometers defined in Fig. 7), this parameter was considered to have a minor influence on the overall response, as failure strains between 6 and 20%, resulted in a 4% difference in peak accelerations, Fig. 6. Increasing element removal reduces peak acceleration, but at the expense of (artificially) increasing case deformation (as becomes weaker) and vice-versa. Strains greater than 20% resulted in element instabilities and significant reduction in calculated timestep by upto two orders of magnitude (i.e. 40% element deletion reached 0.38 ms before prematurely terminating and were disregarded).

**4. Influence of glass and adhesive properties**

For the initial drop presented in Section 2, a 1.8 m drop equates to a velocity of 5.9 ms<sup>-1</sup> and 8.2 J impact energy. Automatic tied penalty based contact algorithms (with contact smoothing) were defined (as debonding not considered initially). Impact surface was represented as a rigidwall. Mass proportional damping assigned, with an appropriate damping factor equivalent to 10% of critical damping [7,8].

Two numerical accelerometers were defined; at the centre of mass (referred to as “Mid”) and 65 mm above this location as per test (referred to as “Upper”), in order to assess influence of accelerometer placement (Fig. 7). Sampling rates of 10 ns and a termination time of 1 ms allowed capturing of peak deceleration and first rebound.

In order to assess model robustness and level of correlation, three sensitivity studies performed:

1. Assess influence of accelerometer position on acceleration time histories.
2. Impact Angle variations around baseline:  $\Delta\theta_z = \pm 5^\circ$ ,  $\Delta\theta_x = \pm 5^\circ$ , and combinations
3. Assess influence of glass and adhesive by investigating the stiffening effects each component has on the metal body-glass interface and overall tablet response.

Nomenclature used to quantify damage is presented in Fig. 8; dimensions ‘a’ and ‘b’ determine major and minor axis of the dent, while ‘c’ represents shortening between diagonally opposite corners. Resultant acceleration time histories and metal body damage are

**Table 5**  
Johnson–Holquist ceramic material properties for silica based glass [6].

Shear modulus (GPa)	A	B	C	m	n	$\epsilon_0$	Tensile strength	Normalised fracture strength	HEL (GPa)	HEL pressure (GPa)	HEL strength (GPa)
30.4	0.93	0.088	0.003	0.35	0.77	1.0	0.15	0.5	5.95	2.92	4.5
Damage constraints			d1	d2	Equation of state			K1 (GPa)	K2 (GPa)	K3 (GPa)	$\beta$
			0.053	0.85				45.4	-138	290	1.0

presented in Fig. 9 and Table 6 respectively.

**4.1. Influence of accelerometer position**

Subtle differences of up to 2.5% observed between accelerometer locations (Fig. 9), with the upper accelerometer predicting higher peak acceleration (2152 g) than centre of mass location (2094 g). For both locations, accelerations are overestimated by ~ +25% when compared to mean test (1723 ± 39g). The initial peak is not sensitive to position ( $t < 0.5$  ms), whereafter, the signals reflect local dynamic effects (metal body vibration) and variations in stiffness (due to packaging of internal components). Therefore, all subsequent FE results will be compared to the Up(per) accelerometer, as per test setup.

**4.2. Influence of impact angle**

As numerical models predict higher peak accelerations when compared to test (> 25%), robustness of the measured acceleration time histories was investigated. An impact angle sensitivity analysis was performed for five additional conditions; namely ± 5° angles applied in plane (global  $\theta_z$ ), out of plane (global  $\theta_x$ ) and their combinations, as based on the right hand rule and coordinate system defined in Fig. 7.

Baseline accelerations are presented in Fig. 10, which shows the effect of small changes in impact angle, resulting in a scatter of ~ 439 g. It can be concluded that varying the impact angle alone does not explain the overestimation in predicted peak decelerations. However, this sensitivity could potentially be exploited in a protective case concept, as inducing rotational motion on impact may be beneficial in reducing peak deceleration.

**4.3. Influence of glass and adhesive**

To investigate how glass and adhesive flexibility/failure affects the metal body-glass interface, results from the following configurations are presented in Fig. 11:

1. Complete removal of glass
2. Upper values of Cyanoacrylate, global element deletion
3. Lower values of Cyanoacrylate, global element deletion
4. Lower values of Cyanoacrylate, local element deletion (at impact corner only)

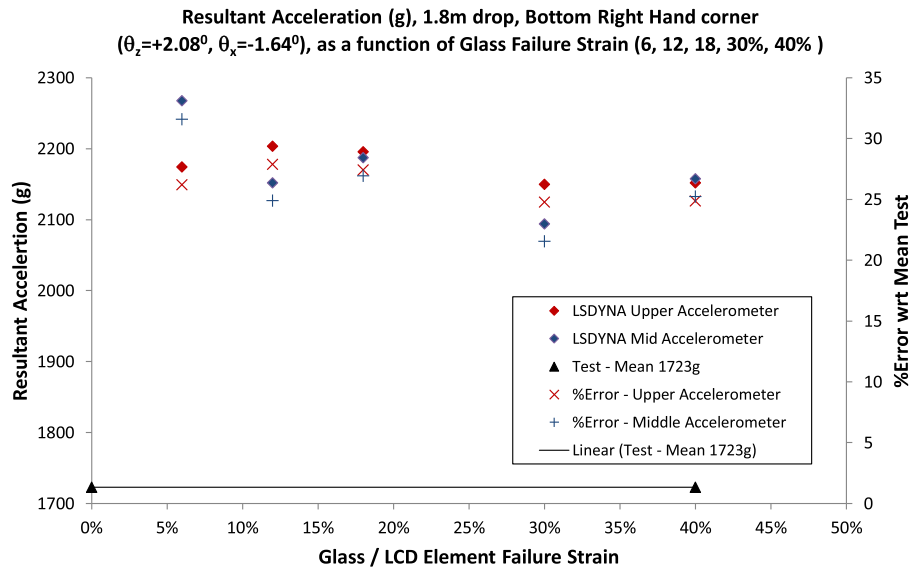


Fig. 6. Influence of glass failure strain (element deletion) on predicted peak decelerations and comparison to test (mean = 1723 ± 39 g).

Removing glass (and reallocating mass) provided a lower bound response and reduced acceleration levels to 1829 g (+6%) when compared to test 1723 ± 39 g. Upper bound values (corresponding to a tied interface), resulted in higher accelerations ~2203 g (+22%), as the perfect bond significantly stiffens the overall response, resulting in minimal deformation and high peak accelerations.

Adhesive was modelled explicitly using TSHELL elements ( $t = 0.25$  mm) and a perfectly plastic material model. As mechanical properties for Cyanoacrylates [9] vary, two extremes were chosen due to uncertainties over the adhesive used by Apple™ (Table 7).

Varying adhesive flexibility and failure reduced peak accelerations to ~9–10% of test (Fig. 11). Using the notation (Adhesive properties, application region of element deletion), peak accelerations predicted were (Upper, global) = 1928 g, (Lower, global) = 1918 g and (Lower, local) = 1897 g.

Failure strain and mechanical properties permit a marginal reduction in peak accelerations, which suggests a change in load distribution between metal body and glass (as adhesive elements deleted at different times). This change in stiffness can be observed by changes in gradient of the acceleration signals in Fig. 11, and demonstrates metal body-glass bonding (and failure) can have a significant influence on predicted accelerations.

### 5. Existing protective cases

Table 8 summarises commercial products (including transportation sleeves) available at the time of this research, which was not exhaustive, but formed a useful starting point in assessing material type and protection mechanism.

Dual material based designs common, as most products use a harder polycarbonate shell dipped in silicone rubber to provide additional cushioning (Hard Candy, Griffin, Otterbox and Gumdrops). The two sleeve cases also use polycarbonate with an elastomer casing (Switcheasy) and a proprietary strain rate sensitive rubber (G-Form). The Otterbox is the only product using internal foam to minimise movement. The final two products (Griffin and Krakken) are substantial cases, designed to meet US-MIL-STD-810F (January 2000) for military and industrial applications [10].

The MIL Standard was originally launched 1962 and the latest revision 810G (October 2008), defines test conditions across twenty nine categories, including shock (vibration and temperature) and environment (moisture, sand, etc) [13]. Section “516.6 -Shock”, procedure IV, stipulates 26 drop tests (5 repetitions per test) from a height of 1.22 m for items weighing <45 kg onto two inches of plywood, backed by concrete. Impact surface will affect damage, as dropping onto plywood is less severe than directly onto concrete, as any localised indentation may reduce impact loading. Only the G-Form sleeve (1 m), Krakken

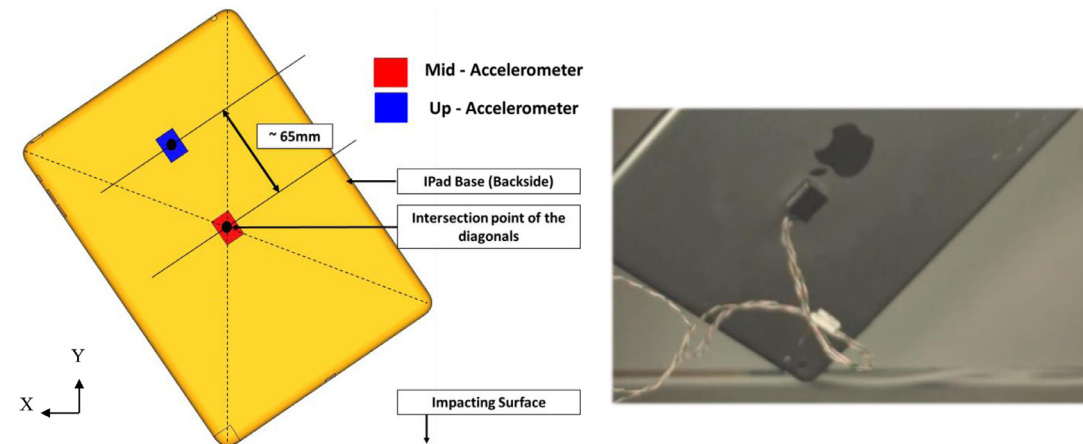


Fig. 7. Definition of Up(per) (65 mm above Apple™ logo) and Mid accelerometers (at centre of mass). (Right image: accelerometer location for top right corner drop).

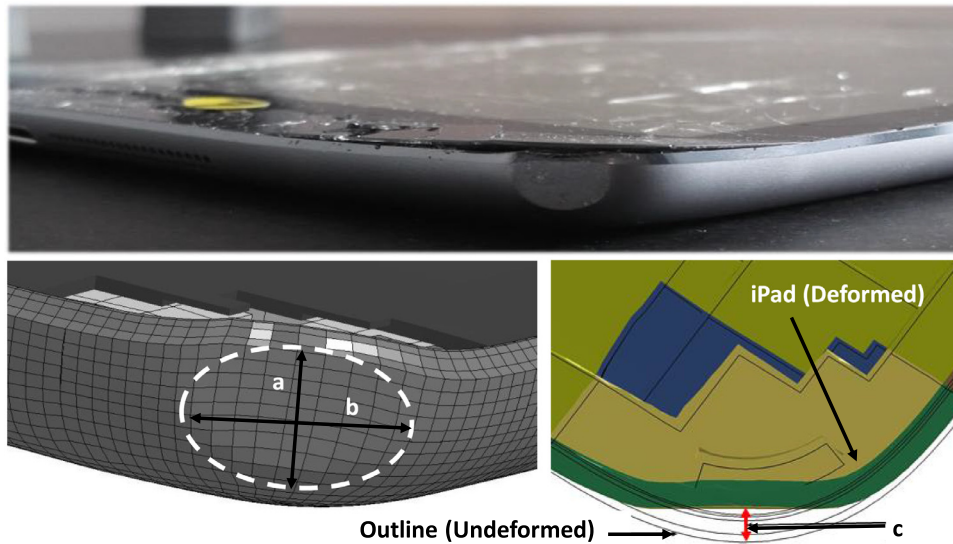


Fig. 8. Parameters used to quantify metal body damage for bottom right hand impact.

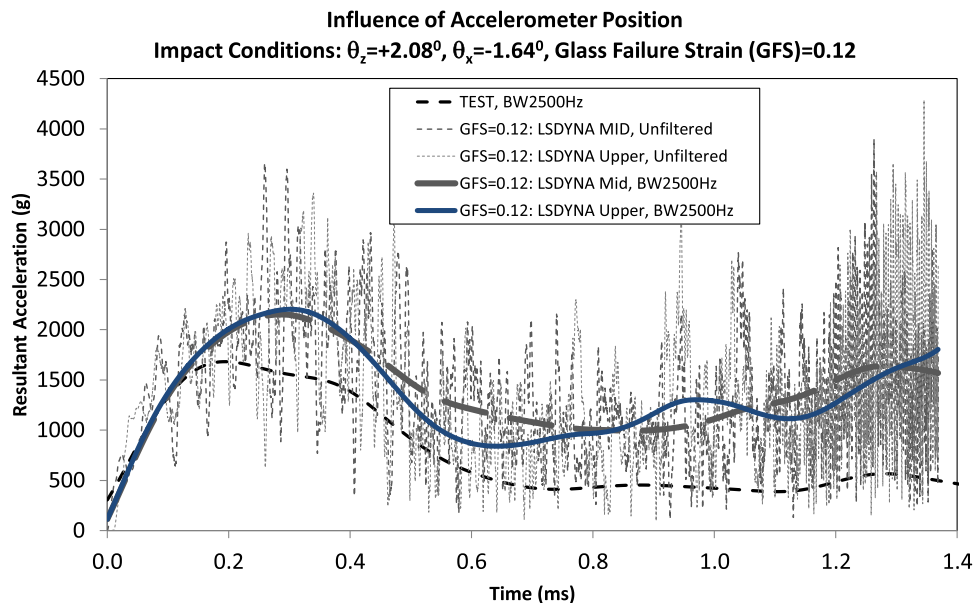


Fig. 9. Baseline resultant acceleration time histories for Mid and Upper accelerometers (Glass/LCD Failure Strain = 0.12%).

**Table 6**  
 Comparison between predicted and experimentally measured deflections.

Bottom right hand corner drop test ( $\theta_z = +2.08^\circ$ , $\theta_x = -1.64^\circ$ )	Dent dimensions (mm)				
	FEA a	b	c	%Error in c	Test c
FE Model (~ 3 h, 8CPUs)					
Intel i7-4810MQ CPU @ 2.8 GHz, 16 Gb RAM	7.60	6.36	1.22	-4.7%	1.28

(1.25 m) and Griffin (1.8 m) specify drop heights, with the Griffin-Survivor offering the best impact protection with a mass of 349 g (~ 80% mass of iPad).

**6. Load by-pass concept: proof of concept**

The research question posed in this paper was whether it was possible to develop a new device independent protection concept sub

200 g, (~ 45% mass of iPad), capable of protecting from a 1.8 m drop onto concrete. This represents a significant design challenge due to the following design constraints:

- Case must represent a book in shape and appearance, completely encapsulating the tablet (with case wrap around limits)
- Maximum 4 mm wall thickness and fixed outer dimensions.
- Apple™ places restrictions on material types to avoid affecting wireless connectivity and signal strength.

Existing designs absorb impact energy through elastic case deformation, typically constructed from compressible foamed materials, or incompressible elastomers. The main disadvantage of this approach is a limit on height protection, as the tablet forms part of the primary load path (and analogous to a single spring-damper system, Fig. 12).

In order to transfer momentum, the concept shown schematically in Fig. 12 and in more detail in Fig. 13, aims to decouple the device from the impact loads by utilising a high in-plane stiffness back plate insert, whose dimensions are larger than the tablet. The device would be



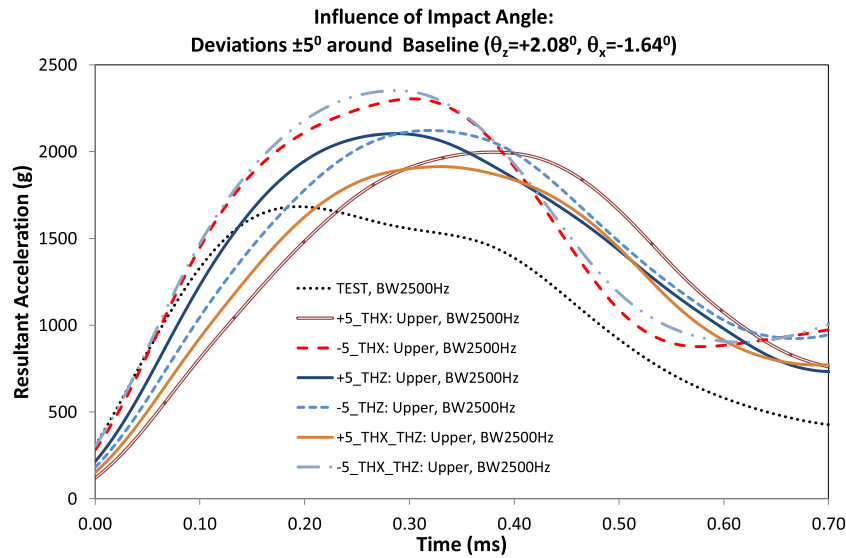


Fig. 10. Influence of impact angle for  $\pm 5^\circ$  variations around  $\theta_x$  and  $\theta_z$  for Bottom right corner drop, with peak accelerations varying by  $\sim 439$  g.

encapsulated by an inner (softer) elastomer, providing localised load alleviation and allowing relative motion between device and case (and analogous to two “springs in parallel”). Decoupling the device will permit decelerations over a longer duration, thereby reducing loading and offering increasing protection across a wider range of drop heights. Key to success is allowing controlled deformation of the inner elastomer. If the elastomer densifies, the tablet would become part of the primary load path, thereby increasing accelerations experienced.

For proof of concept, a 50 ShoreA hardness rubber and a stiffer polycarbonate (PC30) were used for inner and outer cover/back plate respectively, bringing the mass to 163.1 g. Perfect bonding was enforced through tied contacts, taking  $\sim 7$  h (on 16 CPUs, Intel E5 – 2660 CPU) to complete 0.6 ms (sufficient to capture the initial peak deceleration). These materials were chosen as commonly available from elastomer suppliers, in addition to hyperelastic material coefficients available in the literature (Table 9). Two different sets of coefficients were used for comparable hardness rubbers, as parameters for the Yeoh strain energy function [14], (a third degree polynomial allowing the shear modulus to vary with deformation), hereafter referred to as “Yeoh52A”, as coefficients were reported to be stable under large

Table 7

Open source adhesive properties [9].

Component	Young's modulus	Poisson's ratio	Yield stress	Failure strain
Adhesive	10 MPa (lower)	0.3	1 MPa (Lower)	0.01
	1 GPa (Upper)		10 MPa (Upper)	0.10

deformations [15].

Fig. 14 provides a comparison between normalised resultant acceleration for an unprotected and protected tablet, together with the evolution of compression of the inner elastomer. It can be observed:

- Protected tablet develops a relative velocity with respect to the case, due to different acceleration magnitudes and durations. The rigid back plate experiences a higher normalised peak deceleration (1.40 at  $t = 0.15$  ms), which is approximately 1.5 times larger than the tablet (0.91 at  $t = 0.40$  ms), indicating the impact loads are carried by the high stiffness back plate.
- Presence of the cover delays the time the tablet experiences a peak acceleration, which is caused by relative motion between case and

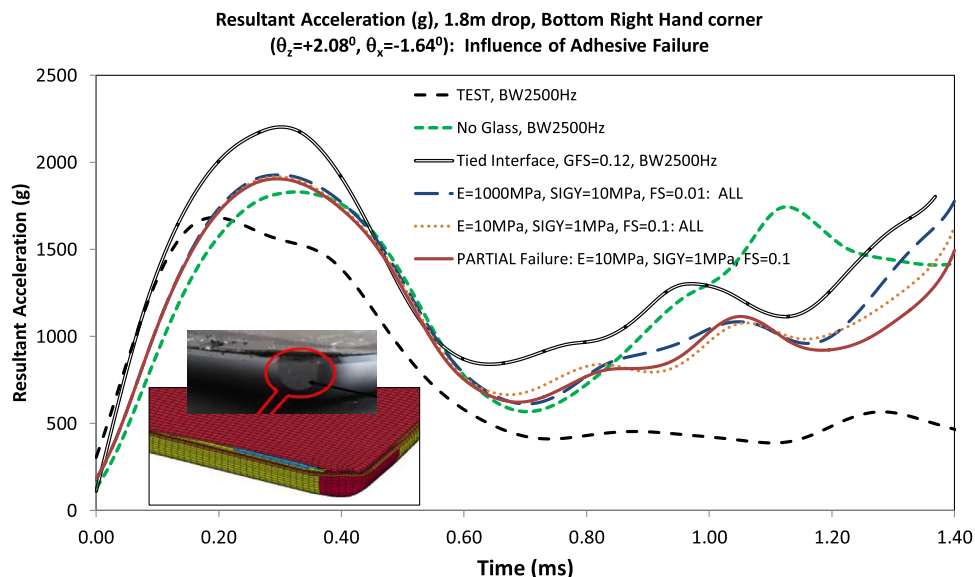


Fig. 11. Influence of adhesive properties and failure (element deletion) on resultant acceleration (Test:  $1723 \pm 39$  g).

**Table 8**  
Commercially available protection cases/sleeves (not exhaustive) [11,12].

Commercial product	Key features
Hard Candy – Case [11]: \$60	<ul style="list-style-type: none"> <li>• Silicone outer skin, Polycarbonate frame</li> </ul>
G-Form – Sleeve [42]: £50	<ul style="list-style-type: none"> <li>• 10 mm extra silicone on corners</li> <li>• Proprietary strain rate sensitive foam, protection up to 1m</li> </ul>
Switcheasy – CARA [43] \$50	<ul style="list-style-type: none"> <li>• Polycarbonate shield, elastomer casing</li> </ul>
Gumdrop cases – Drop Tech [44] 60\$	<ul style="list-style-type: none"> <li>• Reinforce rubber bumpers on corners</li> </ul>
Otterbox Defender [45] \$100	<ul style="list-style-type: none"> <li>• Dual materials for shock absorption</li> <li>• Polycarbonate two-piece internal shell covered in synthetic rubber</li> <li>• Internal foam minimises tablet motion</li> <li>• Rigid polycarbonate shell (six side protection (iPad 2/3/4 only)</li> </ul>
Rokform case [46] \$40	<ul style="list-style-type: none"> <li>• Polycarbonate shell, dipped in silicone</li> <li>• Meets US-MIL-STD-810F (vibration, sand, dust, wind/rain protection)</li> <li>• Rigid internal frame protects against shocks and drops on flat concrete from 6'/1.8 m).</li> <li>• Polycarbonate shell, dipped in silicone</li> </ul>
Griffin – Survivor [47] \$80	<ul style="list-style-type: none"> <li>• Polycarbonate shell, dipped in silicone</li> <li>• Meets/exceeds MIL-STD-810F (vibration, dust, rain and wind protection)</li> <li>• 4 ft impact protection, repels chemicals (acid, household cleaners, etc)</li> </ul>
Krakken [12] (Military version) 80–90\$	<ul style="list-style-type: none"> <li>• Meets/exceeds MIL-STD-810F (vibration, dust, rain and wind protection)</li> <li>• 4 ft impact protection, repels chemicals (acid, household cleaners, etc)</li> </ul>

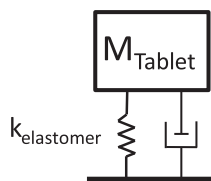
tablet. The peak accelerations occur after ~0.25 ms and ~0.40 ms for unprotected and protected tablet, respectively.

- When the inner elastomer ‘bottoms out’ (i.e. reaches a maximum compression of 1.6 mm), the solid inner elastomer surround offers very high resistance to increased compression, which is reflected by only a 9% reduction in peak acceleration.
- The only practical means of reducing peak acceleration is through careful elastomer design. Inclusion of voids in the inner elastomer surround needs to be optimised to promote a controlled ‘flow’ of rubber (i.e. deformation through shear) in order to avoid ‘bottoming out’ and subsequent (infinite) stiffening.

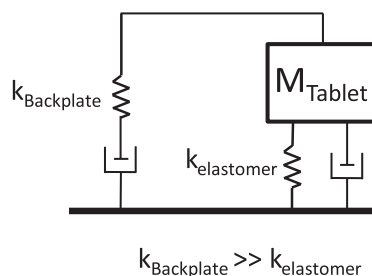
### 6.1. Design variants for elastomeric inner

A systematic exploration was undertaken, which considered the inclusion of recesses in the inner elastomer, either internally or externally, together with different orientations (i.e. along hoop and radial directions). Based on manufacturing considerations (which includes minimum thickness constraints for single pass injection moulding (to ensure quality/repeatability), the aim was to reduce inner elastomer mass by up to 30%, resulting in six variants analysed. All simulations

Tablet **part** of Primary Load Path  
(existing protection concepts)



Tablet **decoupled from** Primary Load Path  
(Proposed protection concept)



utilised the initial material properties in Table 9 and took approximately 10–12 h on 16CPUs (MPP cluster, Intel E5-2660). Key findings are summarised in Table 10, together with normalised resultant accelerations in Fig. 15.

In general, the impact sequence is divided into four stages:

1. *Initial Impact* – all contacts (internal and with impacting surface) established.
2. *Stage I* – Inner elastomer, which is more flexible than the outer cover deforms in shear to fill internal voids. Once the high stiffness back plate makes contact with the impacting surface, the back plate becomes the primary load path.
3. *Stage II* – represents a dwell period, where device moves relative to back plate and is brought to a complete rest by stretching of the inner elastomer. Back plate helps outer cover retain its shape and more importantly, tablet encapsulation.
4. *Rebound* – During rebound, inner elastomer unloads and regains its original dimensions, together with the outer cover retaining its shape.

Based on the normalised acceleration results for variants A–F in Fig. 15:

- Variants A and F offers greatest potential for protection by allowing relative motion to develop between tablet and case (lowering tablet impact velocity and accelerations), through controlled elastomer deformation due to inclusion of internal voids.
- Ensuring sufficient internal space is critical in preventing the inner elastomer contacting the outer case. Preventing bottoming out also minimises chance for the inner elastomer to force the outer case to splay open.
- Outer cover should have sufficient stiffness to resist splaying loads applied through combined action of the inner elastomer and downward tablet motion.
- Variant A was rejected due to potential difficulties in manufacturing, due to a finite bonding area between inner elastomer and outer case/back plate.
- Variant D dismissed based on peak accelerations and manufacturing concerns (I.e. High cost and difficulties in single pass injection moulding).

Variants C, D and F were based upon internal castellations (in hoop and through thickness directions). Based on the findings, castellations in the hoop direction appeared to provide the greatest protection (Variant F), which was taken forward to the prototyping stage for further development.

### 7. Development of the “BLOK™” prototype

The internal geometry of TPE (Thermoplastic Elastomer) voids were

Fig. 12. Spring-damper idealisations of existing protection design (left) and proposed protection concept (right), which decouples the tablet from the primary load path.

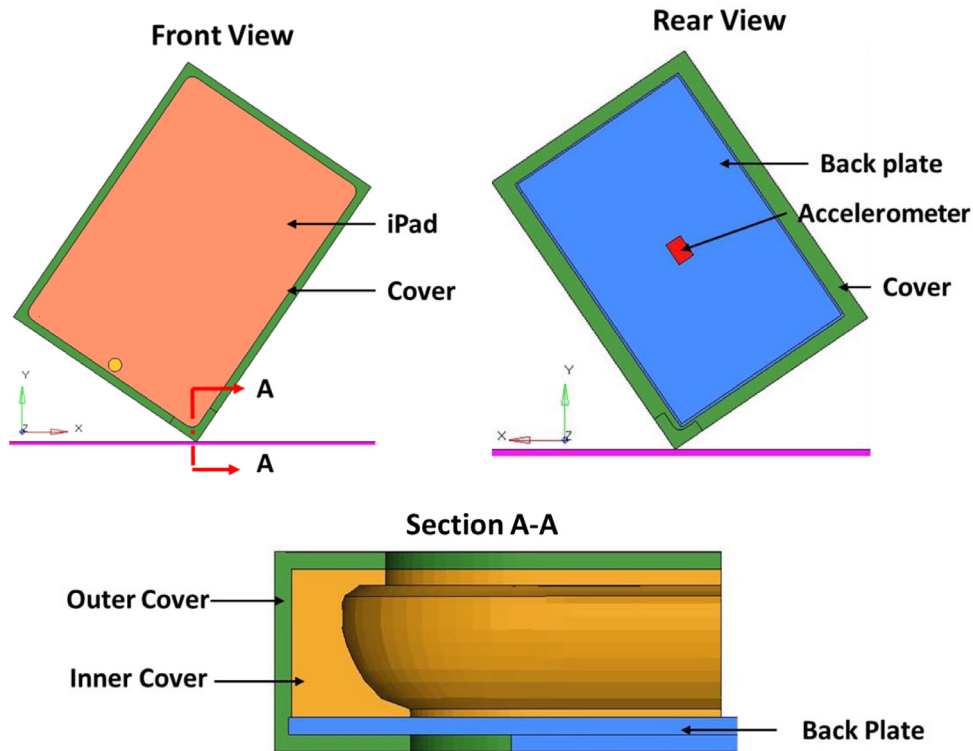


Fig. 13. High stiffness back plate and softer elastomers have the potential to decouple device from the primary load path by allowing relative motion to develop.

Table 9  
Initial material properties (rubber and polycarbonate) [15].

Type	Material model
Incompressible Rubber Shore 50A	*MAT_HYPERELASTIC_RUBBER $\rho = 1100 \text{ kg/m}^3, \nu = 0.499, C10 = 2.45, C01 = -0.54$
Yeoh52A [15]	$\rho = 1100 \text{ kg/m}^3, \nu = 0.495, C10 = 0.55, C20 = -0.05, C30 = 0.95$
Polycarbonate – 30% Carbon filled	*MAT_ELASTIC $\rho = 1320 \text{ kg/m}^3, 20.2 \text{ GPa}, \nu = 0.32$

optimised by considering usability, industrial design and design for manufacture (Fig. 16). Optimised configuration consists of localised, angled castellations, which were discontinuous at each corner to

prevent the inner elastomer bottoming out under a direct corner impact. Along long and short edges, the castellations were orientated normal to the device to provide optimal (distributed) protection from edge impacts. The outer was an 80 Shore A TPE (ThermoPlastic Elastomer), as an increase in stiffness was required to ensure tablet retention, with a less stiff TPE for the inner elastomer. Final case dimensions were  $250 \times 180 \times 11 \text{ mm}$  with a mass of 165 g.

Test programme used a Heina DT2000 Drop Tester [16], whereby attachment was via suction cups which were released prior to impact, allowing repeatable control over impact velocity, point of impact and angle. In all tests, drop height was 1.8 m onto a 17.5 kg concrete slab placed directly onto a concrete floor. High speed cameras (10k frame rate), combined with TEMA Motion analysis software replaced physical accelerometers [17].

Evolution of case response and visual correlation between test and

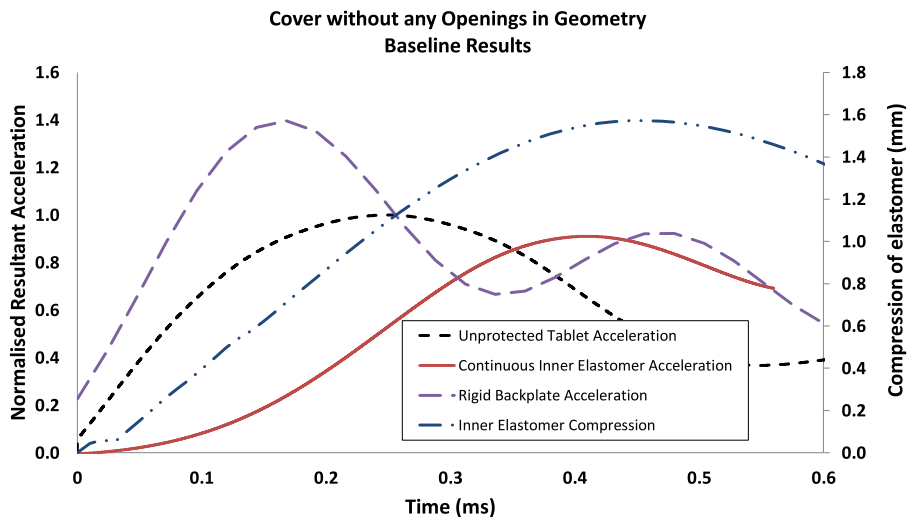
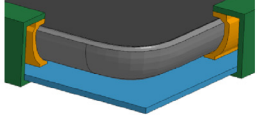
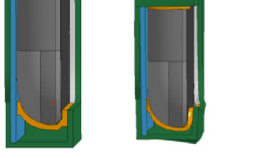
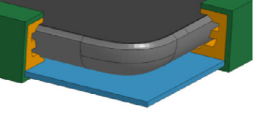
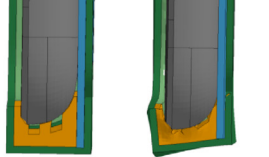
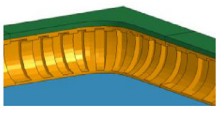
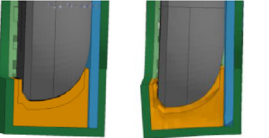
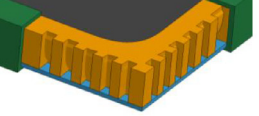
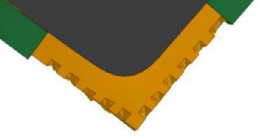
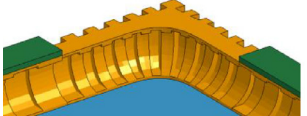
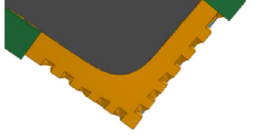
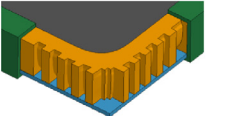
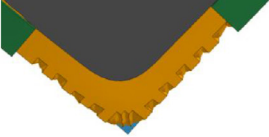


Fig. 14. Normalised resultant acceleration and compression of a solid, continuous inner elastomer for the baseline concept presented in Fig. 13.

**Table 10**  
Different inner elastomer variants.

Concept Variant	Case Response
<p>(A) Outer Grooves, Hoop Direction Mass =150.1g</p> <ul style="list-style-type: none"> <li>• Inner elastomer flows into space/ void created between Inner and Outer cover, minimising case splaying (-35% reduction in peak acceleration).</li> </ul> 	 <p>t = 0ms      t=1.0ms</p>
<p>(B) Inner Grooves, Hoop Direction Mass =193.9g</p> <ul style="list-style-type: none"> <li>• Circumferential grooves increase risk of case splaying due to reduced second moment of area of case along hoop direction (-5% decrease in peak acceleration)</li> </ul> 	 <p>t = 0ms      t=0.5ms</p>
<p>(C) Inner Grooves, Lateral Direction Mass =185.1g</p> <ul style="list-style-type: none"> <li>• -5% reduction in peak acceleration, due bottoming out of inner elastomer (similar issues as Variant B).</li> </ul> 	 <p>t = 0ms      t=0.9ms</p>
<p>(D) Outer Grooves, Lateral Direction Mass =155.1g</p> <ul style="list-style-type: none"> <li>• Corner lug reduces internal space available for inner elastomer, resulting in elastomer bottoming out quickly (+17% increase in peak acceleration).</li> </ul> 	 <p>t=0.6ms</p>
<p>(E) Inner and Outer Grooves - Lateral Direction Mass = 132.0g</p> <ul style="list-style-type: none"> <li>• Similar issue as with Variant D – Inner lateral grooves beneficial, but no net benefit over baseline (+2.3% increase in peak acceleration).</li> </ul> 	 <p>t=0.6ms</p>
<p>(F) Outer Groove, no corner lug - Lateral Direction Mass = 154.7g</p> <ul style="list-style-type: none"> <li>• -29% reduction in peak acceleration, as absence of corner lug allows inner elastomer to deform in shear.</li> </ul> 	 <p>t=0.7ms</p>

simulation is presented in Fig. 17 for a bottom right corner impact. The shape and spacing of the inner castellations performs as expected, cushioning the device. The case distorts at various locations and elastically recovers (Fig. 18), with the device remaining encapsulated throughout the impact event.

Resultant displacement, velocity and acceleration time histories are presented in Figs. 19 and 20, where series 1–4 denote the motion tracking points bonded to the glass screen (Fig. 17).

The kinematics of the tablet are in close agreement in terms of rise time and absolute magnitude, with predicted peak displacement of 8.98 vs 8.45 mm (+ 6%) and close agreement up to 1.8 ms for resultant velocity, whereafter the simulation diverges from test. In terms of resultant accelerations, LSDYNA predicts the rise and fall well, but overestimates the peak deceleration by +14% (509 g vs 447 g at  $t = 1.8$  ms).

The deviations after 1.8 ms suggests LSDYNA overestimates inner elastomer stiffness (at full compression) and its subsequent unloading.

However, the simulation verifies the effectiveness of this proposed concept, as the (predicted) resultant acceleration for an unprotected and protected tablet has been reduced by ~76% (2152 g vs 509 g). This observation is also consistent with test: 1723 g (unprotected) vs 447 g (protected); a 74% reduction. Overall, there is very good agreement to test.

### 8. Final validation case – application to iPad Air 2

During the development of this research, the iPad Air 2 was released, which internally contained many differences to the Air (Table 11). In the Air, the LCD (directly screwed) and outer glass screen (bonded) are attached independently to the aluminium body, decoupling these components through the presence of an internal air gap, thereby reducing the loading experienced by the outer glass. In the Air 2 however, the LCD is bonded directly to the glass screen, making the design slimmer. A direct consequence of this bonding is the outer glass

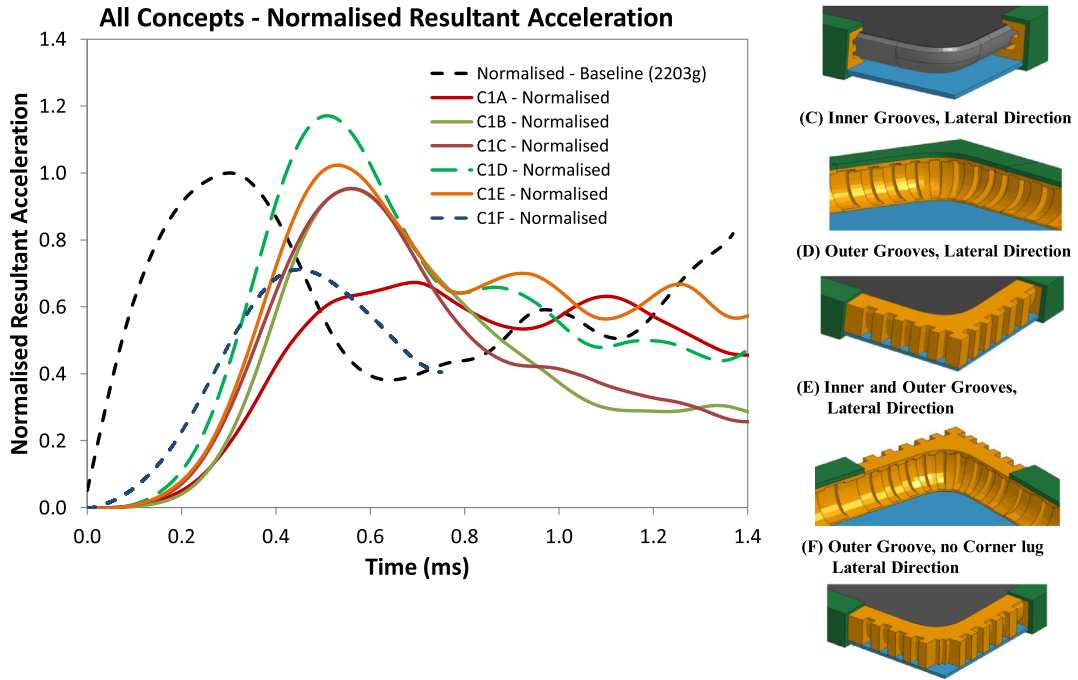


Fig. 15. Normalised resultant accelerations for Concepts A–F.

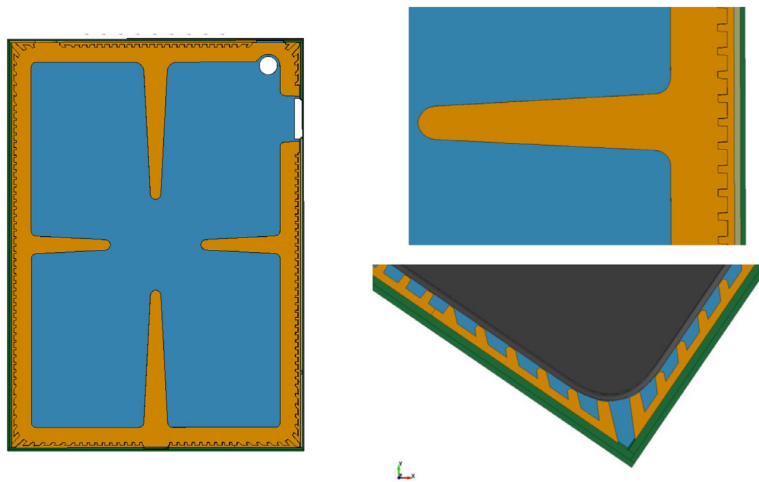
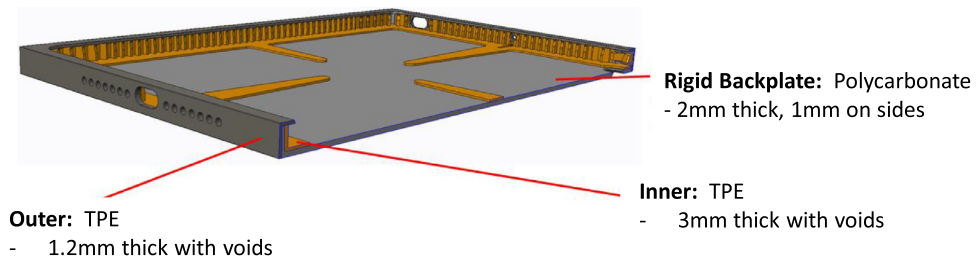


Fig. 16. Finalised BLOK™ protection concept (250 x 180 x 11 mm, mass = 165 g).

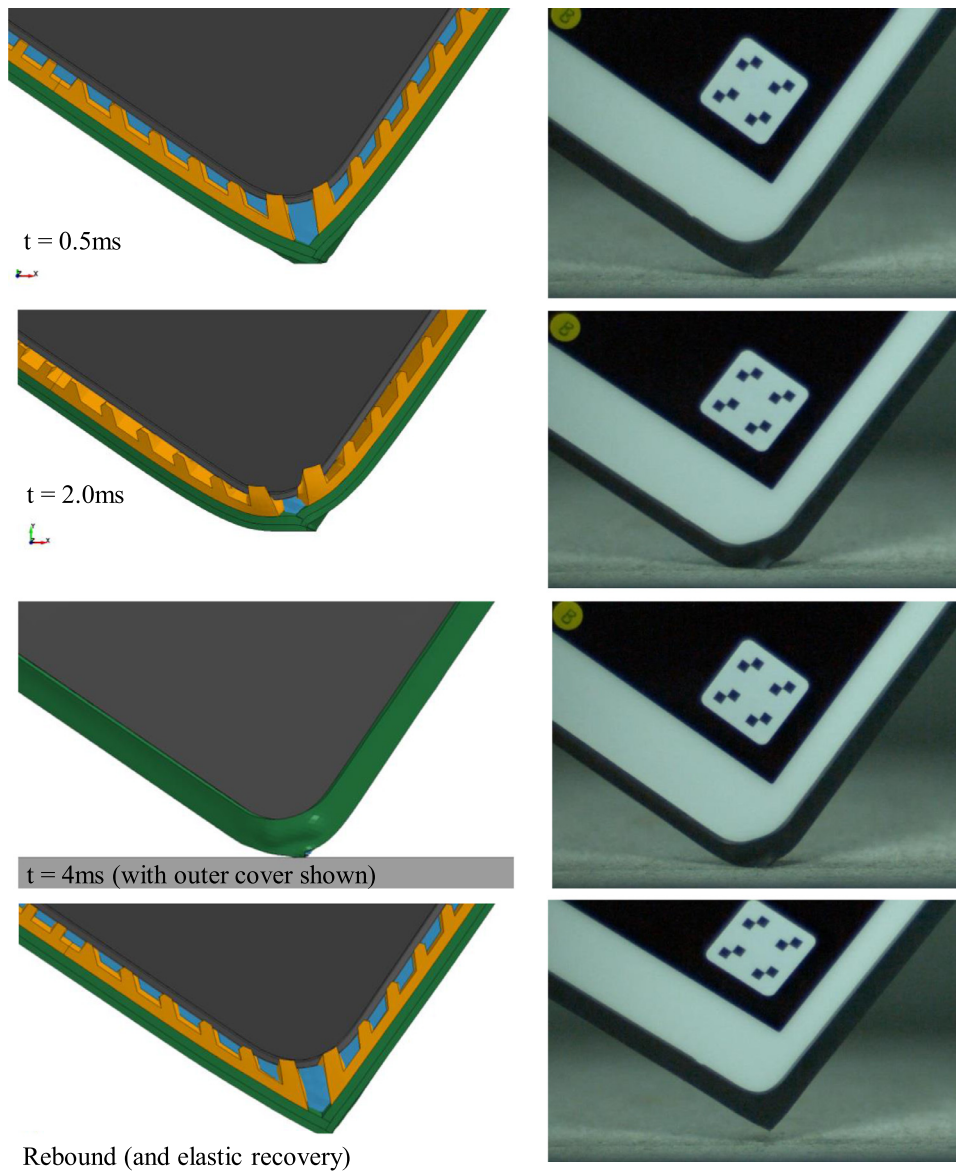


Fig. 17. Test – Simulation correlation, bottom right corner impact, 1.8 m drop onto concrete using a Heina DT2000 guided Drop tester and TEMA motion analysis software.

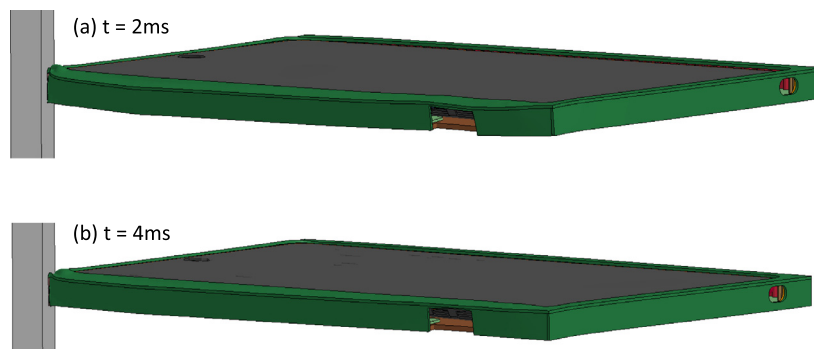


Fig. 18. Peak case distortion (Bottom right corner, 1.8 m drop onto concrete), which shows global case distortions (a) and elastically recovered state (b). Device remains encapsulated throughout impact event.

screen must now support the LCD inertia, making it more susceptible to failure. The corners of the aluminium body have been redesigned, with the Air 2 having less aluminium bulk and potentially more prone to damage.

From physically testing an unprotected Air2, screen damage was

observed during a bottom right corner impact and also for a (distributed) drop along the short edge (Fig. 21). The lower left image clearly shows the empty internal space within the case (and lack of LCD support as it is directly bonded to glass screen), resulting in the glass screen being more prone to cracking/shattering.

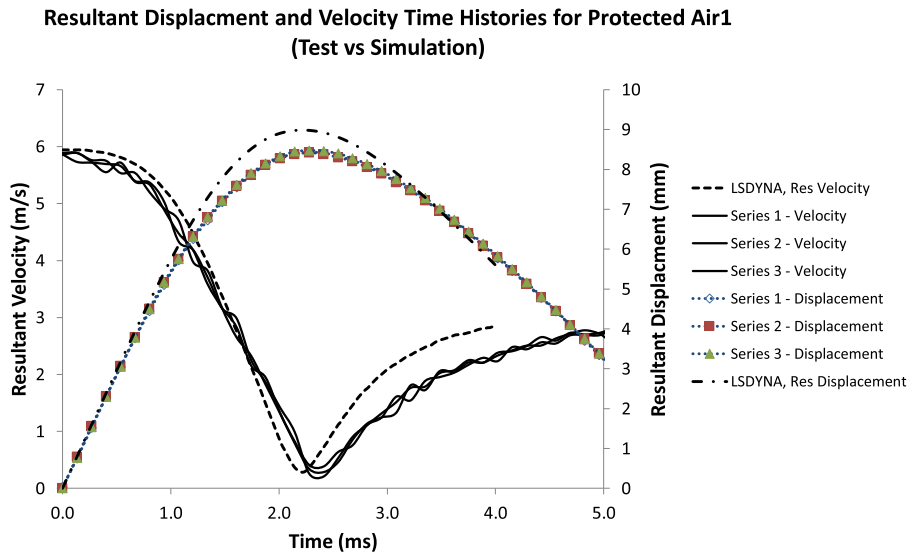


Fig. 19. Test vs simulation: resultant displacement and velocity time histories for protected tablet.

The right images in Fig. 21 are for the tablet protected by the novel protection concept proposed in this research, which clearly demonstrates its effectiveness. The device is fully functional and without any significant damage after testing on all four corners and along all four edges. This is also true when extending the test campaign to consider the remaining twenty six orientations defined in MIL STD-810G. It should be noted that cut outs to the back plate and side walls (for connector, camera, microphone and volume buttons) potentially weaken the cover structure, resulting in case flexure. However, the device is still well protected due to the other elements of the protection system (elastomer castellations and carefully designed corner which increases stopping distance), thereby providing improved protection for all orientations from a 1.8 m drop height onto concrete.

9. Conclusions

- A high fidelity finite element model of an iPad Air was developed to support the analysis led design of a novel protection concept (BLOK™), which utilises different grades of elastomer and optimised internal castellation geometry.
- Glass-metal body bonding (and failure) are key parameters that can affect the overall table response, which would require additional characterisation to align simulation to test.
- Decoupling the tablet from the impact loads has significant

advantages and the potential to provided increased protection to any device (or mobile phone) from even greater drop heights, as the primary load path is through a high stiffness backing plate (not the device).

- The developed model verifies the effectiveness of this concept, as the (predicted) resultant acceleration for an unprotected and protected tablet was reduced by ~76% (2152 g vs 509 g), and consistent to test: 1723 g (unprotected) vs 447 g (protected); a 74% reduction. Displacements agree within 6% and peak acceleration was overestimated by 14% and attributed to LSDYNA overestimating elastomer stiffness at full compression and its subsequent unloading.
- Further validation of the proposed protection concept was demonstrated with the Air2 test campaign, where the tablet was fully functional and without any significant damage after testing on all four corners and along all four edges.
- The proposed concept resulted in a product to market (BLOK™) which complies with aesthetic and mass constraints imposed by Logitech and achieved with a product mass of 165 g (< 200 g design constraint), providing improved protection for all orientations from a 1.8 m drop onto concrete, far exceeding MIL-STD-810G requirements.

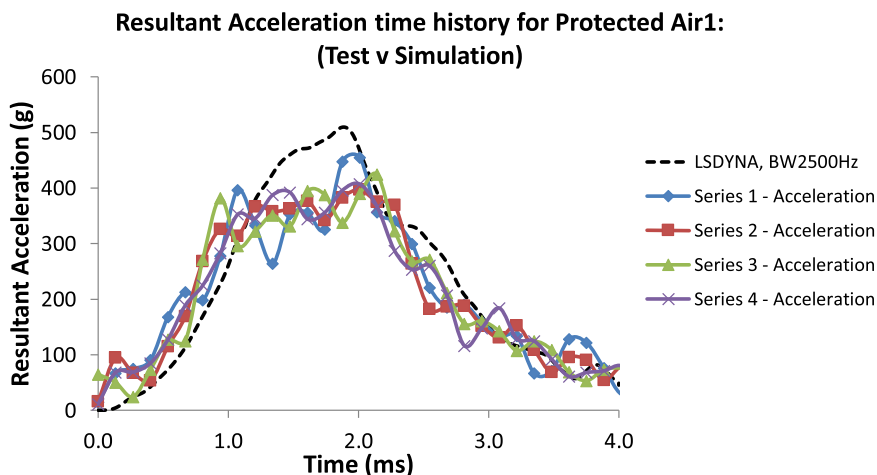






Fig. 20. Test vs simulation: resultant accelerations for protected tablet.

**Table 11**  
Internal differences between iPad Air and Air 2 [18,19].

 <p>LCD directly attached to aluminium body (and decoupled from outer glass screen) – Air [17].</p>	 <p>LCD directly bonded to outer glass screen (coupled) - Air 2 [18]</p>
 <p>Corner case thickness – Air [17]</p>	 <p>Reduced corner thickness– Air 2 [18]</p>

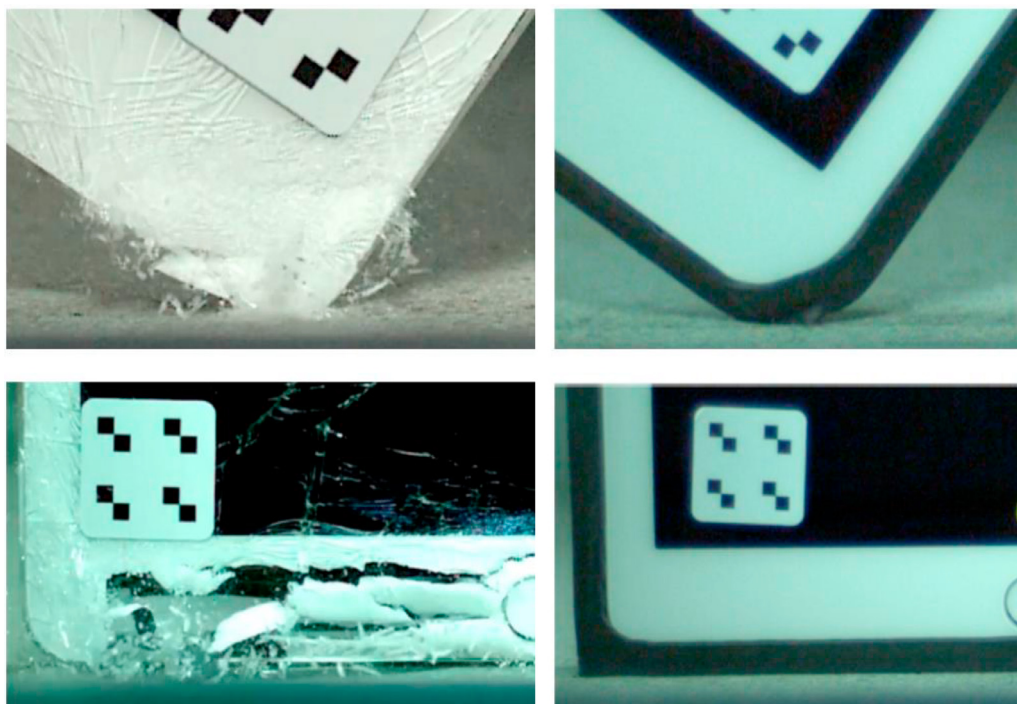


Fig. 21. Experimental testing with and without the proposed protective case concept for an iPad Air 2 dropped from 1.8 m onto smooth concrete.

**Acknowledgements**

Kevin Hughes would like to acknowledge Cranfield University (UK) for enabling part of this research to be performed. The authors would also like to express their thanks to the following Logitech staff, Steve Harvey, Jerry Ahern, Pierce Brady, Ken Delaney and Pdraig Murphy, for their technical contribution.

For further information on BLOK™ (launched August 2015): <http://www.logitech.com/en-gb/blok>.

**Funding**

This research did not receive any specific grant from funding

agencies in the public, commercial, or not-for-profit sectors.

**Supplementary materials**

Supplementary material associated with this article can be found, in the online version, at [doi:10.1016/j.ijimpeng.2018.03.001](https://doi.org/10.1016/j.ijimpeng.2018.03.001).

**References**

- [1] “Apple Website,” 2017. Available: <https://www.apple.com/uk/newsroom/>.
- [2] LSTC. LS-DYNA keyword user's manual – volume 1 (R7.0). Livermore Software Technology Corporation (LSTC); 2013.
- [3] Hallquist J. “LS-DYNA theory manual,” Livermore Software Technology Corporation (LSTC), 2006.



- [4] Corning, “Gorilla Glass,” Corning, [Online]. Available: <https://www.corninggorillaglass.com/>.
- [5] Cronin DS, Bui K, Kaufman C, McIntosh G, Berstad T. Implementation and validation of the Johnson–Holmquist ceramic material model in LS-DYNA. Proceedings of the 4th European LS-DYNA user conference. 2005.
- [6] “Damping Recommendations,” LS-DYNA Support, [Online]. Available: <http://www.dynasupport.com/howtos/general/damping>. [Accessed 11.10.17].
- [7] Gulavani O, Hughes K, Vignjevic R. Explicit dynamic formulation to demonstrate compliance against quasi-static aircraft seat certification loads (CS25.561) – part I: influence of time and mass scaling. *Proc Inst Mech Eng Part G J Aerosp Eng* 2014;228(11):1982–95.
- [8] Hwan C-L, Lin M-J, Lo C-C, Chen W-L. Drop tests and impact simulation for cell phones. *J Chin Inst Eng* 2011;34:337–46.
- [9] US-MIL-810F. Department of defense test method standard for environmental engineering considerations and laboratory tests. Department of Defense; 2000.
- [10] Hard Candy Cases, Hard Candy, [Online]. Available: <http://www.hardcandycases.com/device/ipads/ipad-air-cases/shockdrop-poptop-case-for-ipad-air.html>.
- [11] “Kraken Military Edition A.M.S Case,” Trident, [Online]. Available: <http://www.tridentcase.com/shop-products/apple-ipad-air/military-edition-kraken-ams-case-apple-ipad-air.aspx>. [Accessed Feb 2017].
- [12] US-MIL-STD-810G. Department of defense test method standard for environmental engineering considerations and laboratory tests. Department of Defense; 2008.
- [13] Yeoh O. Characterization of elastic properties of carbon-black-filled rubber vulcanizates. *Rubber Chem Technol* 1990;63(5):792–805.
- [14] Oscar J, and Centeno G. “Finite element modeling of rubber bushing for crash simulation – experimental tests and validation,” Master’s Dissertation – ISSN 0281-6679, Lund University.
- [15] “High-class drop testing (meets MIL-STD-810G, Method 516.5),” Heina, [Online]. Available: <http://www.heina.net/droptester/>. [Accessed February 2016].
- [16] TEMA Motion, “The leading motional analysis suite,” [Online]. Available: <http://www.imagesystems.se/index.php/download/public/tema/motion/Product-Sheet-TEMA-Motion.pdf>. [Accessed February 2016].
- [17] [www.ifixit.com](http://www.ifixit.com), “Air teardown,” [Online]. Available: <https://www.ifixit.com/Teardown/iPad+Air+LTE+Teardown/18907>. [Accessed June 2016].
- [18] [www.ifixit.com](http://www.ifixit.com), “Air2 Teardown,” [Online]. Available: <https://www.ifixit.com/Teardown/iPad+Air+2+Teardown/30592>. [Accessed July 2016].
- [19] Suhir E, Burke R. Dynamic response of a rectangular plate to a shock load, with application to portable electronic products. *IEEE Trans Compon Packag Manuf Technol Part B* 1994;17(3):449–60.
- [20] Nagaraj B. Drop impact simulation of a custom pager product. *Adv Electron Packag* 1997;1:539–74.
- [21] Goyal S, Upasani S, Patel D. Improving impact tolerance of portable electronic products: case study of cellular phones. *Exp Mech* 1999;39(1):43–52.
- [22] Goyal S, Upasani S, Patel D. Role of case rigidity in drop-tolerance of portable products. *Int J Microcircuits Electron Packag* 1999;22(2):175–9.
- [23] Low K, Yang A, Hoon K, Zhang X, Lim J, Lim K. Initial study on the drop-impact behaviour of mini Hi-Fi audio products. *Adv Eng Softw* 2001;32(9):683–93.
- [24] Lim C, Low Y. Investigating the drop impact of portable electronic products. Proceedings of the electronic components and technology conference. 2002. 28–31 May.
- [25] Seah S, Lim C, Wong E, Tan V, Shim V. Mechanical response of PCBs in portable electronic products during drop impact. Proceedings of the 4th electronics packaging technology conference. 2002. 10–12 December.
- [26] Lim C, Teo Y, Shim V. Numerical simulation of the drop impact response of a portable electronic product. *IEEE Trans Compon Packag Technol* 2002;25(3):478–85.
- [27] Lim C. Drop impact survey of portable electronic products. Proceedings of the electronic components and technology conference. 2003.
- [28] Low K. Drop-impact cushioning effect of electronics products formed by plates. *Adv Eng Softw* 2003;34(1):31–50.
- [29] Low K, Wang Y, Hoon K, Vahdati N. Initial global-local analysis for drop-impact effect study of TV products. *Adv Eng Softw* 2004;35(3–4):179–90.
- [30] Lye S, Lee S, Chew B. Virtual design and testing of protective packaging buffers. *Comput Ind* 2004;54(2):209–21.
- [31] Yi J, Park G. Development of a design system for EPS cushioning package of a monitor using axiomatic design. *Adv Eng Softw* 2005;36(4):273–84.
- [32] Wang H, Chen S, Huang L, Wang Y. Simulation and verification of the drop test of 3C products. Proceedings of the 8th international LS-DYNA user conference. 2004. 2–4 May.
- [33] Tan V, Tong M, Lim K, Lim C. Finite element modeling of electronic packages subjected to drop impact. *IEEE Trans Compon Packag Technol* 2005;28(3):555–60.
- [34] Cadge D, Wang H, Bai R. Drop test simulation of electronic devices using finite element method. Proceedings of the international conference on electronic materials and packaging, EMAP 2006. 2006.
- [35] Shan H, Su JZJ, Xu L. Three-dimensional modeling and simulation of a falling electronic device. *J Comput Non-Linear Dyn* 2007;22(2).
- [36] Pan M, Chen P. Drop simulation and experimental validation of TFT-LCD monitors. Proceedings of the 5th conference on electronics packaging technology, (EPTC 2003). 2004.
- [37] Yu D, Kwak JB, Park S, Lee J. Dynamic responses of PCB under product-level free drop impact. *Microelectron Reliab* 2010;50(7):1028–38.
- [38] G. Grewolls, and A. Ptchelintsev, “Robustness evaluation of mobile phone drop test simulation – NOKIA,” 2010. [Online]. Available: [http://www.dynardo.de/fileadmin/Material\\_Dynardo/bibliothek/WOST\\_7.0/Presentation\\_Grewolls.pdf](http://www.dynardo.de/fileadmin/Material_Dynardo/bibliothek/WOST_7.0/Presentation_Grewolls.pdf).
- [39] Altair Press Release, “Altair and LG electronics slash smartphone drop-test simulation time from weeks to less than 24 hours,” December 2013. [Online]. Available: [http://www.altair.com/NewsDetail.aspx?news\\_id=10919&AspxAutoDetectCookieSupport=1](http://www.altair.com/NewsDetail.aspx?news_id=10919&AspxAutoDetectCookieSupport=1).
- [40] Blanco D, Ortalda A, Clementi F. Impact simulations on home appliances to optimize packaging protection: a case study on a refrigerator. Proceedings of the 10th international LS-DYNA user conference. 2015.
- [41] “G-Form protective sleeve,” G-Form, [Online]. Available: <http://www.g-formuk.com/products.html>.
- [42] Switch easy, [Online]. Available: [http://www.switcheasy.com/product/CARA\\_ThenewiPad](http://www.switcheasy.com/product/CARA_ThenewiPad).
- [43] Gumdrop, [Online]. Available: <http://www.gumdropcases.com/device/ipads/ipad-air-cases/drop-tech-case-for-ipad-air.html>.
- [44] Otterbox, [Online]. Available: <http://www.otterbox.com/ipad-air-cases/ipad-air-cases,default.sc.html>.
- [45] “iPad 2/3/4 shield case,” Rokform, [Online]. Available: <http://www.rokform.com/roklock-v3-ipad-case/>.
- [46] “Griffin survivor,” griffin technology, [Online]. Available: <https://griffintechnology.com/us/survivor-all-terrain-for-ipad-air-2>. [Accessed February 2017].
- [47] Seogggwan K, Wonjoon C. Simulation of the drop test of a packaged refrigerator. *Reliab Stress Anal Fail Prev* 1995;87:109–16.